

# Extent of Saltwater Intrusion and the Freshwater Exploitability in the Coastal Vietnamese Mekong Delta. A Case Study in Ham Luong estuary

Pham Thi Bich Thuc<sup>1\*</sup>, Do Anh Dao<sup>1</sup>, Nguyen Tan Trung<sup>1</sup>, Dang Nguyen Nha Khanh<sup>1</sup> and Nguyen Trung Nam<sup>2</sup>

<sup>1</sup> Institute of Applied Mechanics and Informatics, Vietnam Academy of Science and Technology, Ho Chi Minh 700000, Vietnam

<sup>2</sup> Southern Institute for Water Resources Planning, Ministry of Agriculture and Rural Development, Ho Chi Minh City, Vietnam

**Abstract.** Climate change-driven sea level rise has intensified saltwater intrusion in deltas worldwide, posing significant threats to the exploitation of freshwater resource. In the Vietnamese Mekong Delta, the third largest delta globally, saltwater intrusion is degrading freshwater resources and affecting socio-economic development in the long run. In this paper, we investigate the spatiotemporal extent of salinity intrusion in the Ben Tre Province, the hotspot of salinity disaster is 2021. Long-term salinity monitoring data (1996–2022) has been analyzed, and 3D hydrodynamic model (Mike 3) was Our results indicated that salinity patterns are well-stratified at the beginning and end of the dry season but well-mixed during the middle period. Over the course investigated periods, SI has started progressively earlier in the dry season and increased over the last year. Over the course investigated periods, SI has started progressively earlier in the dry season and increased over the last year. Modeling for SI have also revealed a growing complexity in exploiting freshwater resources, manifesting as challenges related to timing, depth, and geographic location.

## Key word:

Mekong; salinity; projection; climate change; freshwater

## 1 Introduction

Saltwater intrusion is the phenomenon of saltwater from the sea encroaching into the mainland during high tides and is especially large during the dry season, causing many difficulties in the exploitation and use of freshwater resources in rivers. Saltwater intrusion is becoming increasingly complex due to the impact of climate change and is a matter of concern in water resource management in estuarine deltas around the world [1]. In the future, estuarine deltas will face many risks of increased saltwater intrusion due to the impact of socio-economic development such as industrial and agricultural pollution, changes in mainstream flow due to climate change and the development of hydroelectric dams [2]. Climate change and sea level rise scenarios predict that drought and saltwater intrusion will increase [3]. Hydrological droughts in river basins will reduce the amount of freshwater in the main river, causing saltwater to move further upstream, increasing the area of saltwater intrusion. Sea level rise is also expected to increase the level of erosion as increased sea pressure will push saltwater further inland. In this context, direct human impacts such as increased demand for irrigation and multi-purpose freshwater exploitation aggravate saltwater intrusion, especially in areas facing freshwater scarcity and salinity [4]. Freshwater in coastal estuaries is quite limited and fluctuates seasonally while the demand for fresh water is increasing due to population explosion and agricultural, industrial and domestic production processes serving economic and technological development [5]. This increase is also the result of land use changes serving economic development, changing the natural environment of the basin [6]. In 2015, water crisis was identified as the main risk to the global economy as 50% of the world's population living within 200 km of the coast faced challenges from seasonal water shortages, saltwater intrusion and over-exploitation of groundwater. Freshwater storage solutions are often built reservoirs [7] and desalinated seawater into freshwater. These solutions are often very expensive and difficult to implement because they occupy a large surface area but are susceptible to environmental pollution due to saltwater intrusion. Therefore, flexible and sustainable solutions are urgently needed to minimize saltwater intrusion and help exploit freshwater in coastal estuaries.

---

\* Corresponding author: [ptbthuc@iami.vast.vn](mailto:ptbthuc@iami.vast.vn)



## 2.2 Hydraulic modeling approach and data

### 2.2.1 Model setup

This study applied and Mike 3 (3D) from Mike Hydro model software developed by Danish Hydraulic Institute (DHI). Model simulation based on Navier–Stoke equation system for incompressible free flow under shallow water based on Boussinesq assumption. Mike 3 is a three-dimensional visualization of hydrodynamic, diffusion, and ecological processes for marine areas, estuaries, in rivers and lakes. In terms of hydrodynamics, the interactive processes of currents and tides, processes stratification, ocean currents, thermal circulation, and salt diffusion are simulated (Soudi et al., 2019). Mike 3 model was applied to simulate the salinity structure characteristics in the vertical and horizontal directions of the Tien river mouth during the dry season, at the beginning, middle, and end of the season. The grid was built for the main rivers of the Tien river tributary, including Co Chien, Ham Luong, Cua Tieu, and Cua Dai Rivers. On the ocean domain, the model network extended 30km to the sea and was 96km wide. The grid consisted of a total of 14,859 nodes with 17,122 grid points, and the grid size in the offshore area was about 1.5 - 2km. The closer to the shore, the smaller the grid size, varying from 200 - 500m, while the mesh size in the river varied from 20 - 100m. The model had four (04) boundaries, including one (01) upstream and three (03) from the sea side. The vertical stratification was divided into seven (07) layers, and the descriptive roughness coefficient varied spatially in the domain.

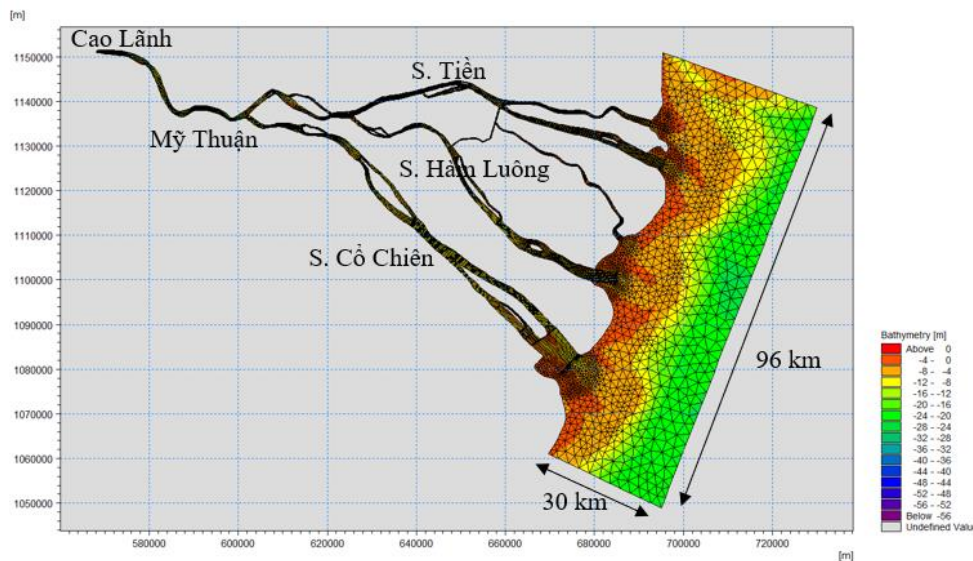
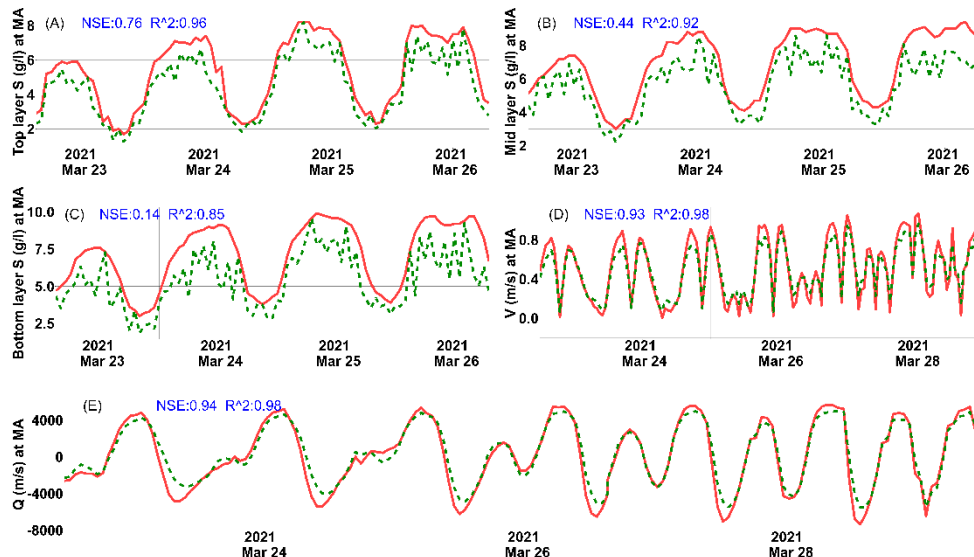


Figure 2 : Grid calculation of the study area model

The Nash-Sutcliffe coefficient (NSE) and the correlation coefficient R are used to evaluate the performance and reliability of the simulation models. Nash-Sutcliffe coefficient (NSE). The developed model showed relevant performance in calibration and validation over the dry seasons of 2021 (Table 2). Our results indicate that the model and actual measurement results are highly correlated with R<sup>2</sup> and NSE between 0.44 and 0.95 figure 3.



**Figure 3.** Observed and simulated data comparisons at My An (MA) station in March of 2021 (A) surface salinity, (B) middle layer salinity, (C) bottom salinity, (D) velocity, and (E) discharge.

### 2.2.2 Data availability

In this study, we analyzed measured salinity data of four (04) stations of An Thuan, Son Doc, My Hoa along the Tien River (Ham Luong) to evaluate the salinity distribution structure over the 1996–2022 period. We measured salinity concentration at My An on Ham Luong river from March 21st to 31st, 2021 to calibrate and verify the Mike 3 model. Salinity concentrations were measured by depth at cross-sections and along the river using CTD–272 salinity meters while the velocity and discharge were monitored by Acoustic Doppler Current Profiler (ADCP, RDI Workhorse 600 kHz).

### 2.2.3 Determining the salinity extent and structure

In the estuary, salinity is distributed and structured according to depth, hence it is necessary to determine the disturbance form according to three forms, including salt wedge, partial disturbance and total disturbance. The formula for determining the disturbance forms in the estuary was conducted firstly by studies of Pritchard, (1967). In theory, salt wedges form when the amount of freshwater flowing into the estuary is greater than the tidal flow. Partial turbulence is a freshwater current that is above the salty tidal current. When the high tide forces the upper freshwater flow, the salinity layers increase with the water flow to the sea. Total disturbance occurs when the flow in the river is small and tidal currents play a major role. In our study, we analyzed salinity data over 25 years (1996–2022) at An Thuan, Son Doc, My Hoa, stations from the river mouth to the mainland (5.29 – 45 km from the coast) to understand the distribution and structure of salinity along the Tien River (Co Chien estuary) in time and space. In estuary areas, the tides are active, and the water in the river shows the basic changes in salinity over time.

The following equation is applied to determine the distribution of salinity along the Tien river (Ham Luong estuary) in the form of saline intrusion:

$$n = \frac{\Delta S}{S_m} = \frac{S_{bottom} - S_{surface}}{0.5(S_{bottom} + S_{surface})} \quad \text{eq.1}$$

Where: S is the difference between bottom and surface salinity.

S<sub>m</sub> is average salinity.

S<sub>bottom</sub> and S<sub>surface</sub> are bottom and surface salinity.

When there is a strong disturbance and weak stratification ( $n < 0.1$ ); partial shuffle and moderate stratified and weak shuffle ( $0.1 < n < 1$ ); and strongly stratified ( $1 < n < 2$ ). Notably, the value of n never exceeds 2.

### 2.2.4 Identifying salinity threshold for freshwater exploitation

To determine solutions of freshwater exploitation, our study applied salinity standard for domestic water of 0.2g/l by the Ministry of Health according to the regulations of the Vietnam Ministry of Health No. QCVN 01-1:2018/BYT and surface water quality standards No. QCVN 08-MT:2015/BTNMT with the salinity in surface water from 0.25–0.35g/l. In addition, Ben Tre Plantation and Plant Protection Sub-Department have recommended the salt tolerance threshold of plants sensitive to salinity less than 1g/l (rambutan, durian, mangosteen), low salinity threshold of 2g/l (rice, corn, oranges, tangerines), average salinity threshold of 2–3g/l (tomatoes, peppers, cucurbits, bananas, sugarcane, grapefruit, lemons) and high salinity threshold of 3–4g/l (mango, jackfruit, soursop, and coconut). We use these thresholds to assess the model results of scenarios in combination with water balance calculations which help to propose solutions to adapt and deal with the saline intrusion.

## 3 Result

### 3.1 Evaluation of the analysis results of the salinity distribution structure

The annual average salinity over the period 1996–2022 at three(03) stations decreases from the estuary to the upstream in ranges of 0.3–31.5g/l at An Thuan (near the river mouth) (Figure 4A), 0.1–28.2g/l at Son Doc (Figure 4B), 0–17.2g/l at My Hoa (Figure 4C). The reduction in average salinity between stations compared with An Thuan by the ratio of Son Doc–An Thuan 57 %, My Hoa– An Thuan 85%, reflects that the discharge in the river is the main factor determining the salinity level at each location. However, this is a very sensitive estuary, in the low salinity year 2014 salinity at Son Doc decreased by 65%, My Hoa decreased by 100%. In the high salinity year 2016, Son Doc salinity decreased by 13%, My Hoa decreased by 65%. Although the salinity values highly fluctuate, the average daily salinity for many years is relatively low (Figure 4D). Average daily salinity at An Thuan station (5.49km from the sea) is only 12.7g/l, Son Doc (4.2 g/l),

Giong Trom (1.5g/l), and My Hoa (1.3g/l). The trend of average daily salinity distribution shows that the location of freshwater exploitation is favorable for domestic use and agricultural production at a position 25km from the sea. In general, the variation of salinity depends on the tidal cycle, the freshwater discharge upstream and the location. Our calculation results of the average daily, daily salinity distribution for each month from January to July and its mean in the dry season over the period of 1996 - 2022. The salinity levels along the Ham Luong River at four (03) stations start to increase from January and peak in March or April before gradually decreasing in May and ending in July. The constraint time for freshwater exploitation at the salinity level of 0.3g/l is about 6 months at An Thuan, and Son Doc station, 5 months at Son Doc. The time of freshwater exploitation at An Thuan is only 0 - 20 hours mainly in June and July, 0-145 hours at Son Doc in January and February, and up to 180 hours in June or July. For a salinity level of 4g/l, the limited time for freshwater exploitation is much better, with 5 months at An Thuan, 4 months at Son Soc, and 1 month in Huong My and Tra Vinh. The number of hours that freshwater can be exploited at An Thuan is from 0 - 148 hours, 0 - 356 hours at Son Doc, respectively.

Table 1: presents the difference in salinity of the surface–bottom layer and the coefficient  $n$  to determine the structural forms of saline intrusion according to measured data of the three (03) stations. Calculation results show that  $n < 0.1$  is the largest,  $n > 0.1$  accounts for about 50% of the times  $n < 0.1$  while the least times is of  $n > 1$ . Therefore, the saline intrusion structure of Ham Luong estuary is classified as evenly disturbed–weakly stratified.

Table 1: Differences in surface and bottom salinity and coefficient  $n$  at three stations

$\Delta S$	AN Thuận		Sơn Đốc		Mỹ Hóa	
	$\Delta S$	time	$\Delta S$	Time	$\Delta S$	Time
<b>&lt;0.1</b>	684	3258	3426	4215	96	98
<b>&gt;0.1</b>	784	1470	1301	306	276	274
<b>&gt;1</b>	1694	71	94	1	0	1

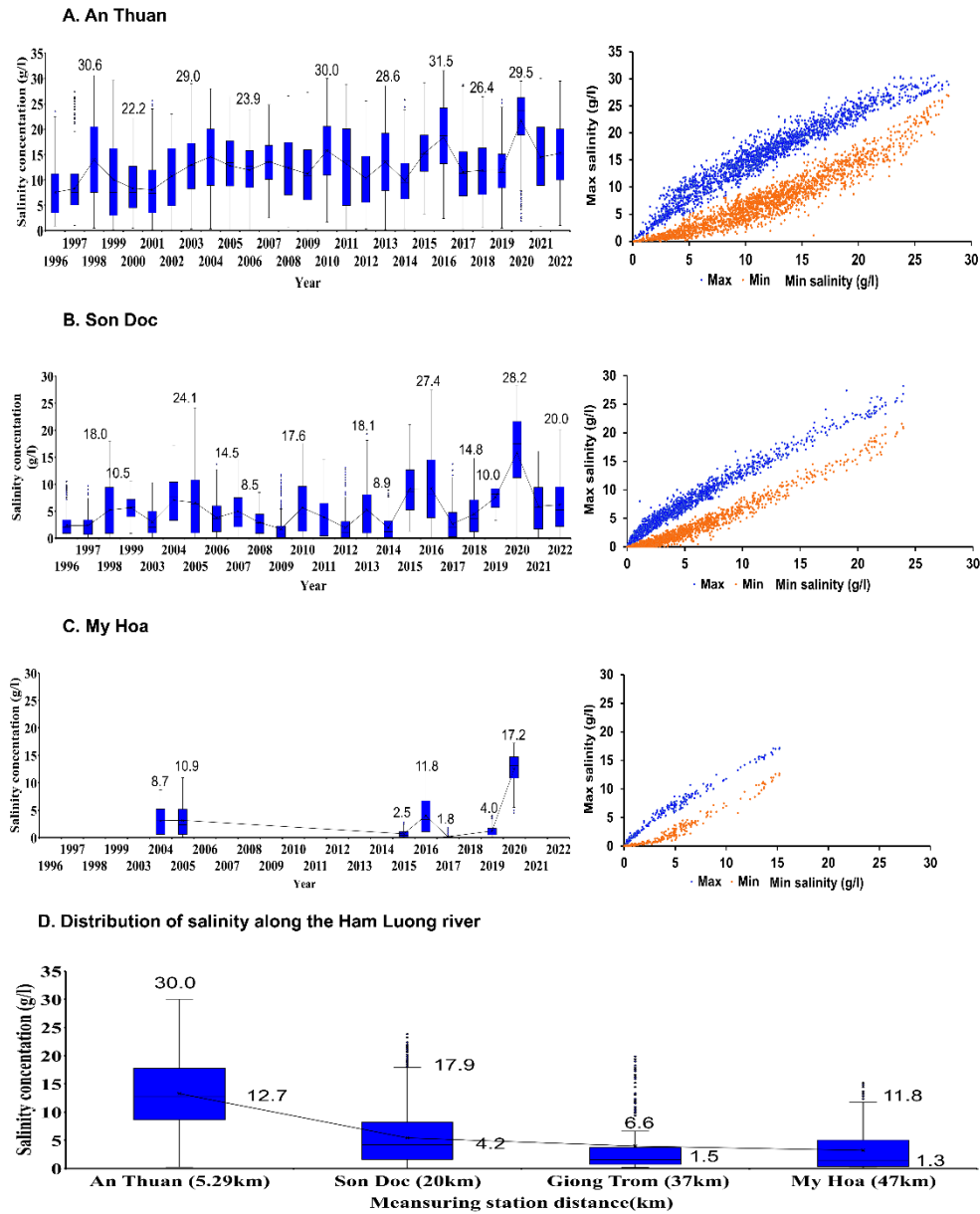


Figure 4: Salinity evolution by year in the period 1996-2022 and distribution of max and min values at (A) An Thuan, (B) Son Doc, (C) My Hoa. Distribution of salinity along the Ham Luong River (D).

### 3.2 Modeling result (3D)

Distribution of saline intrusion structure along the Tien River from Co Chien estuary upstream to My Thuan station (IP14) is presented using the Mike 3 model simulation results for the beginning - middle - end of the dry season in 2021 (Figures 5, 6, and 7).

At the beginning of the dry season, at the time of rising tide and salinity well mixed at the estuary nearly 15km from the sea, the possible freshwater exploitation locations are 70km from the sea (Figure 5). At the low tide phase, the freshwater extraction site is 40km from the sea. Our analysis of salinity structure in cross-section shows that when the tide is high, the distribution of salinity is skewed to the right bank and deeper (Figure 5B). When the tide is low, there is no flow layering, the salinity disturbance is uniformly distributed vertically according to different values from the left bank to the right bank (Figure 5C). The ability to take freshwater according to the cross-sectional layering in the middle of the dry season is not feasible.

In the middle of the dry season, the structure of saline intrusion is evenly disturbed at high tide and stratified at low tide (Figure 8). During the phase of high tide, salinity is mixed evenly from the estuary to the 47km position upstream (IP 11), hence freshwater cannot be exploited at all three (03) locations of An Thuan (5.49km), Son Doc (20km), My Hoa (47km). During the low tide phase, strong disturbances form and weak stratification, freshwater can reach 36 km away

from the estuary. However, considering the vertical depth (Figure 6C), the freshwater layer at 22km (IP 6) is very thin, the exploitable location well ranges from 30km upstream. The cross-sectional salinity structure distributes salinity in the middle of the section at high tide and layered at low tide. The saline layer is close to the river bottom, so the upper freshwater layer can be taken at a depth of 1 - 2m.

At the end of the dry season, salinity stratifies along the river at both high and low tide phases (Figure 7). When the tide rises, the salinity intrudes further upstream and stratifies in the estuary position of 6 km, and evenly distributed at a position 36km from the sea. The time of low tide is limited to stratification from the estuary to 20km and the surface freshwater appears at Son Doc (20km). The cross-sectional evolution is evenly mixed at the high tide (Figure 7B) and stratified at the low tide (Figure 7C). The time to extract freshwater at low tide at the end of the dry season is favorable, the exploitable freshwater layer is 3m.

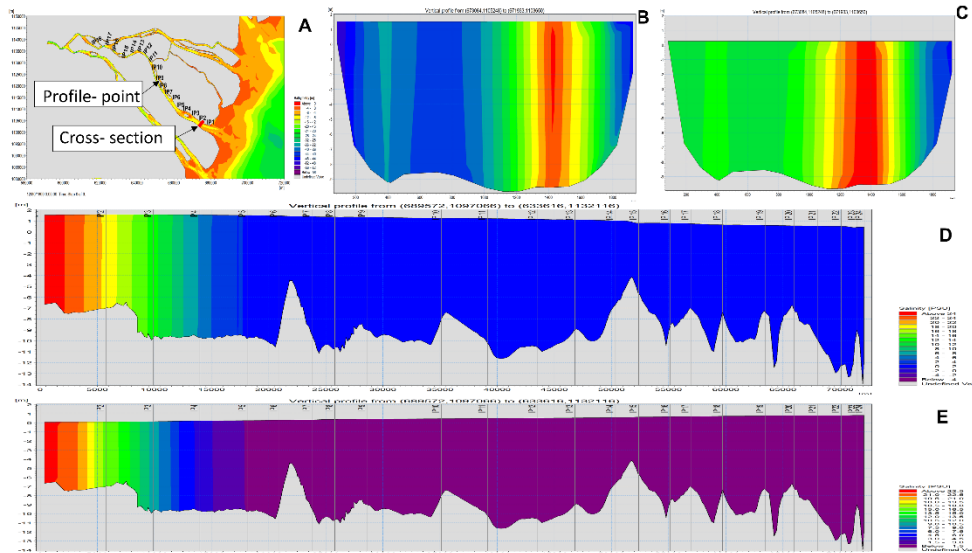


Figure 5: Distribution of salinity along the river and at the typical cross-section at the beginning of the dry season. (A). River identified profile point (IP) and typical cross-sectional location; (B) Salinity at the cross-section at high tide; (C) Salinity at the cross section at low tide; (D) Salinity along the river at high tide; (E) Salinity along the river at low tide.

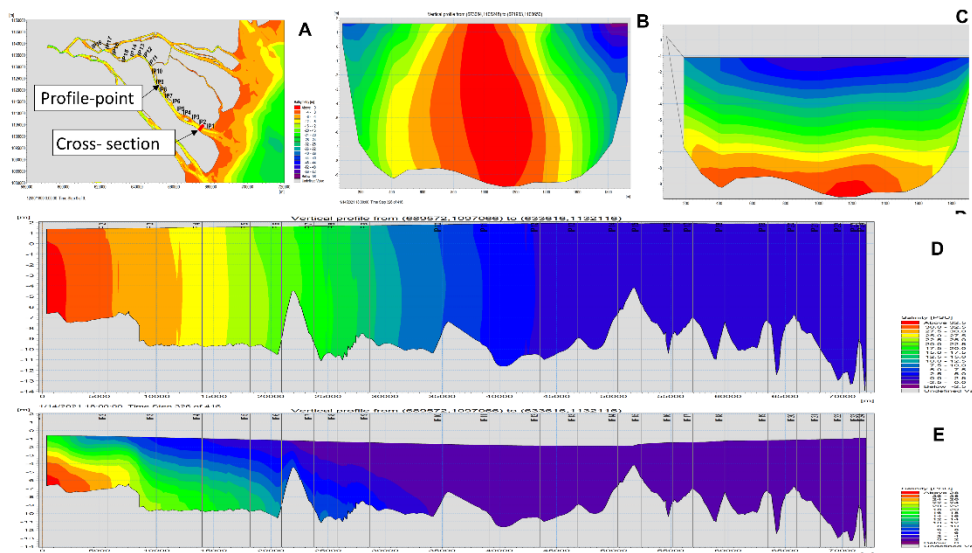


Figure 6. Distribution of salinity along the river and at the typical cross-section in the middle of the dry season. (A). River identified profile point (IP) and typical cross-sectional location; (B) Salinity at the cross-section at high tide; (C) Salinity at the cross section at low tide; (D) Salinity along the river at high tide; (E) Salinity along the river at low tide.

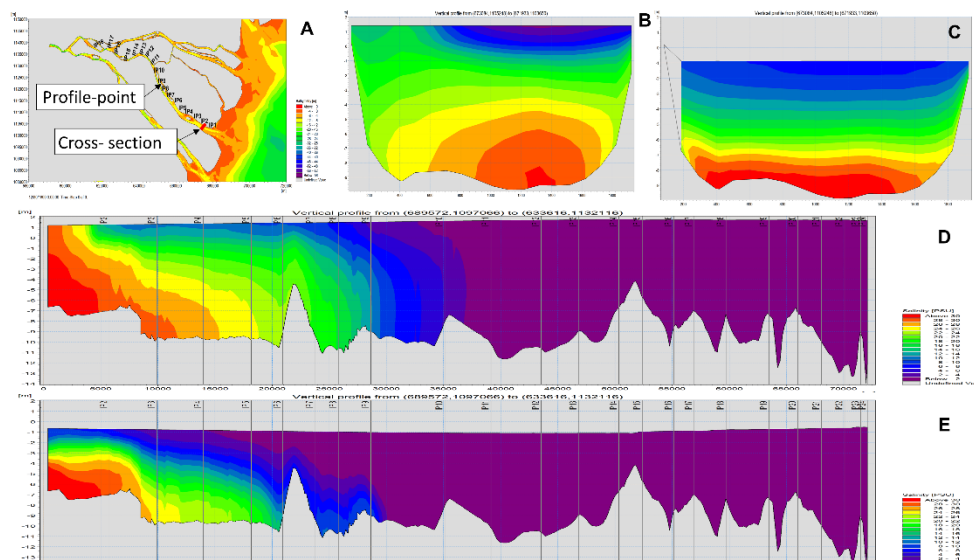


Figure 7: Distribution of salinity along the river and at the typical cross-section at the end of the dry season. (A). River identified profile point (IP) and typical cross-sectional location; (B) Salinity at the cross-section at high tide; (C) Salinity at the cross section at low tide; (D) Salinity along the river at high tide; (E) Salinity along the river at low tide.

## 4 Conclusion

This study aims to investigate the spatial and temporal distribution, vertical structure, and mechanism of saline intrusion in Ham Luong estuary in the Vietnamese Mekong Delta. Specifically, monitoring data from 1996 to 2022 are analyzed in conjunction with simulations 3D model (Mike 3) to understand the distribution and mechanism of salinity intrusion and propose solutions for freshwater exploitation in the dry season. The tides and discharge upstream of the river are the two main drivers of salinity distribution in the main river. Over the period of 1996–2022, the tides intrude further inland in years with less water upstream that withdraw freshwater. The salinity structure along the river and cross-section changes over time according to three typical shapes of stratified salinity in the early and late seasons, partially disturbing the mid-season period. Hence, it requires a strict schedule for freshwater exploitation in the early and the late time period of the dry season at suitable locations (30-50km depending the salinity concentration levels) and depths (1-3m).

## References

- [1] G. B. Noe, K. W. Krauss, B. G. Lockaby, W. H. Conner, and C. R. Hupp, “The effect of increasing salinity and forest mortality on soil nitrogen and phosphorus mineralization in tidal freshwater forested wetlands,” *Biogeochemistry*, vol. 114, no. 1–3, pp. 225–244, Jul. 2013, doi: 10.1007/s10533-012-9805-1.
- [2] C. J. Anderson and B. G. Lockaby, “SEASONAL PATTERNS OF RIVER CONNECTIVITY AND SALTWATER INTRUSION IN TIDAL FRESHWATER FORESTED WETLANDS,” *River Res Appl*, vol. 28, no. 7, pp. 814–826, Sep. 2012, doi: 10.1002/RRA.1489.
- [3] C. Prudhomme et al., “Hydrological droughts in the 21st century, hotspots and uncertainties from a global multimodel ensemble experiment,” *Proc Natl Acad Sci U S A*, vol. 111, no. 9, pp. 3262–3267, Dec. 2013, doi: 10.1073/PNAS.1222473110.
- [4] I. Haddeland et al., “Global water resources affected by human interventions and climate change,” *Proc Natl Acad Sci U S A*, vol. 111, no. 9, pp. 3251–3256, Mar. 2014, doi: 10.1073/pnas.1222475110.
- [5] J. Schleich and T. Hillenbrand, “Determinants of residential water demand in Germany,” *Ecological Economics*, vol. 68, no. 6, pp. 1756–1769, 2009, Accessed: Dec. 21, 2022. [Online]. Available: <https://ideas.repec.org/a/eee/ecolect/v68y2009i6p1756-1769.html>
- [6] Y. Sun, S. T. Y. Tong, M. Fang, and Y. J. Yang, “Exploring the effects of population growth on future land use change in the Las Vegas Wash watershed: an integrated approach of geospatial modeling and analytics,” *Environ Dev Sustain*, vol. 15, no. 6, pp. 1495–1515, Dec. 2013, doi: 10.1007/S10668-013-9447-Z.
- [7] J. Liu, S. Yang, and C. Jiang, “Coastal Reservoirs Strategy for Water Resource Development—A Review of Future Trend,” *J Water Resour Prot*, vol. 05, no. 03, pp. 336–342, 2013, doi: 10.4236/JWARP.2013.53A034.
- [8] S. Eslami et al., “Dynamics of salt intrusion in the Mekong Delta: Results of field observations and integrated coastal-inland modelling,” *Earth Surface Dynamics*, vol. 9, no. 4, pp. 953–976, Aug. 2021, doi: 10.5194/esurf-9-953-2021.